Equilibrium charge states of swift F ions after passage through thin foils: Projectile-velocity dependence and target-atomic-number dependence

K. Shima, T. Ishihara, T. Miyoshi, T. Momoi, and T. Mikumo
Tandem Accelerator Center, University of Tsukuba, Ibaraki 305, Japan
(Received 15 August 1983)

Equilibrium charge-state distributions of F ions have been measured in the collisions of (1) (29—108)-MeV F+C and (2) 30- and 60-MeV F + $_{Z_2}X$ foils. Measurement (1) is done to investigate the projectile-velocity dependence of the mean charge state, distribution width, and charge-distribution function. Measurement (2) is done to investigate the Z_2 (target atomic number) dependence of F-ion charge states using 20 kinds of foils with different Z_2. Contrary to the Z_2 oscillation of mean charge states of swift Si and Cl ions, obvious Z_2 oscillatory behavior has not been observed in 30- and 60-MeV F ions. Generally, higher-charge states are observed after passage through lower-Z_2 foils, which follows a trend similar to the Z_2 dependence of effective charges estimated from stopping powers.

I. INTRODUCTION

In the study field of ionic charge states observed behind thin foils, recent interests are mostly focused on finding some systematics with respect to the ionic atomic number Z_1, target atomic number Z_2, or ionic velocity v. Lennard *et al.* found the systematic variation of mean charge states of $Z_1=5$—26 ions after passage through carbon foil,[1,2] Z_2 oscillation of mean charge states was observed by Shima *et al.* for Si and Cl ions[3] and by Harumaya *et al.* for He ions.[4] On the other hand, based on the recent data of various heavy ions, Shima *et al.* obtained a new empirical formula of mean charge states that is useful in the swift ion velocity region,[5] and Baudinet-Robinet proposed the charge-distribution function which is applicable to any velocity of ions after passage through carbon foil.[6]

In this work, considering the above features, equilibrium charge states of swift F ions have been measured from two different aspects. One is to investigate the ion-velocity dependence of charge state over the wide range of ion velocities. At present, charge distributions of (29—108)-MeV F ions after passage through carbon foil have been observed. Comparing the data with those of Almqvist *et al.* taken below 28 MeV,[7] the mean charge state, charge-distribution width, and charge-distribution function have been analyzed in the light of current empirical relations. The second purpose of this work is to investigate the Z_2 dependence of F-ion charge states. For this purpose, 20 kinds of foils with different Z_2 have been irradiated with 30- and 60-MeV F ions. As the result, higher-charge states have been observed for F ions after passage through lower-Z_2 foils.

II. EXPERIMENTAL PROCEDURE AND RESULT

The detail of the experimental procedure is described in a paper by Ishihara *et al.*[8] ^{19}F ions supplied by the tandem accelerator at the University of Tsukuba passed through a thin foil. The ions with charge state q were analyzed with a magnetic spectrograph and their beam current was integrated. A surface-barrier semiconductor counting the elastically scattered F ions served as a monitor to determine the charge-state fraction $F(q)$. Foils used to investigate the Z_2 dependence were Be, C, Mg, Al, KCl, Ti, Cr, Fe, Ni, Cu, Ge, Zr, Mo, Ag, Sn, Sm, Yb, Au, Pb, and Bi. Except for foils of Ge and KCl, self-supporting foils were used. For foils of Ge and KCl, evaporation was done on a 5-μg/cm^2 carbon backing, and the backing side was placed at upstream of the incident beam. The foil thickness was estimated from the measurement of α-particle energy loss using an ^{241}Am source. For the thickness of thin carbon foils, absolute values were estimated from the combination of absolute measurement of 30—148 μg/cm^2 through an α-particle energy-loss method and relative measurement of 3—148 μg/cm^2 through the detection of elastically scattered F ions.

In the equilibrium charge-distribution measurement,

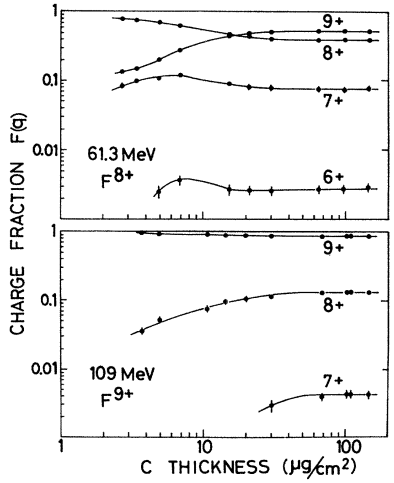

FIG. 1. Nonequilibrium charge-state fractions $F(q)$ of F ions after passage through carbon foils for the incidences of 61.3-MeV F^{8+} and 109-MeV F^{9+}.

TABLE I. Equilibrium charge-state fraction $F(q)$ of ^{19}F ions after passage through carbon foil.

Incident energy (MeV)	Exit energy (MeV)	Foil thickness ($\mu g/cm^2$)	Mean charge $\bar{q}$	Distribution width d	Charge-state fraction $F(q)$ (%) 5+	6+	7+	8+	9+
30	28.7	132	7.47	0.80	0.55	8.83	42.9	38.9	8.86
40	38.9	132	7.88	0.77	0.11	2.89	27.1	48.3	21.6
50	49.0	132	8.20	0.72		0.94	15.1	47.4	36.6
60	59.1	132	8.42	0.65		0.28	8.23	40.9	50.6
61.3	60.3	148	8.45	0.64		0.25	7.37	39.3	53.1
70	69.2	132	8.57	0.58		0.09	4.26	33.8	61.9
80	79.2	132	8.70	0.51			2.26	25.6	72.1
90	89.3	132	8.76	0.46			1.37	21.0	77.6
95	94.3	132	8.80	0.43			0.95	18.4	80.6
109	108.3	148	8.86	0.36			0.42	13.0	86.6

TABLE II. Equilibrium charge-state fraction $F(q)$ of ^{19}F ions with incident energies of 30 and 60 MeV after passage through various foils.

Incident energy (MeV)	Exit energy (MeV)	Foil	Foil thickness ($\mu g/cm^2$)	Mean charge $\bar{q}$	Distribution width d	Charge-state fraction $F(q)$ (%) 5+	6+	7+	8+	9+
30	28.6	Be	156	7.77	0.83	0.35	5.30	31.7	43.8	18.9
	28.7	C	132	7.47	0.80	0.56	8.83	42.9	38.9	8.86
	28.5	Mg	196	7.39	0.79	0.69	9.87	45.6	37.2	6.69
	28.8	Al	164	7.43	0.80	0.73	9.65	43.7	38.1	7.36
	28.6	KCl	220	7.28	0.78	1.02	12.4	49.4	31.9	5.20
	28.5	Ti	243	7.20	0.73	0.93	12.7	55.6	27.2	3.51
	28.9	Cr	189	7.24	0.72	0.77	11.1	54.6	30.3	3.22
	28.4	Fe	287	7.24	0.74	0.89	11.8	53.3	30.4	3.61
	28.8	Ni	229	7.25	0.75	0.86	12.1	52.1	30.9	3.95
	29.3	Cu	133	7.23	0.78	1.20	13.9	49.7	31.3	3.93
	29.1	Ge	169	7.22	0.80	1.42	14.4	49.1	30.7	4.34
	28.3	Zr	377	7.21	0.77	1.23	13.6	51.9	29.4	3.89
	28.2	Mo	410	7.21	0.77	1.27	13.9	51.1	29.8	3.83
	29.2	Ag	188	7.20	0.72	0.96	12.3	56.1	27.4	3.17
	28.8	Sn	293	7.27	0.72	0.85	10.7	55.7	29.5	3.30
	29.2	Sm	234	7.35	0.80	0.97	11.1	46.2	35.4	6.28
	29.2	Yb	242	7.27	0.81	1.38	13.5	47.1	32.6	5.43
	29.5	Au	166	7.18	0.80	1.60	15.1	51.1	27.9	4.24
	29.5	Pb	175	7.20	0.78	1.77	13.3	51.9	29.3	3.79
	28.8	Bi	436	7.14	0.73	0.84	15.0	56.4	24.7	2.99
60	59.0	Be	156	8.63	0.57		0.11	4.02	29.0	66.9
	59.1	C	132	8.42	0.65		0.28	8.23	40.9	50.6
	58.9	Mg	196	8.25	0.70		0.58	13.5	46.6	39.4
	59.1	Al	164	8.25	0.70		0.64	13.3	46.5	39.5
	58.9	KCl	220	8.24	0.71		0.62	14.3	45.2	39.8
	58.8	Ti	243	8.14	0.73		1.08	17.1	48.9	32.9
	59.0	Cr	189	8.11	0.72		1.09	17.9	49.6	31.4
	58.7	Fe	287	8.10	0.72		0.97	18.5	50.0	30.5
	59.0	Ni	229	8.09	0.72		0.99	18.7	50.3	30.0
	59.4	Cu	133	8.06	0.73		1.28	20.2	49.8	28.7
	59.3	Ge	169	8.08	0.73		1.28	19.2	49.5	30.0
	58.6	Zr	377	8.10	0.73		1.30	18.4	49.5	30.8
	58.5	Mo	410	8.12	0.73		1.18	17.8	48.7	32.3
	59.4	Ag	188	8.02	0.74		1.69	21.5	50.1	26.8
	59.1	Sn	293	8.00	0.74		1.66	22.3	50.2	25.9
	59.1	Sm	303	8.12	0.72		0.98	17.9	49.1	32.0
	59.4	Yb	242	8.13	0.74		1.24	17.7	47.7	33.4
	59.6	Au	165	8.03	0.75		1.92	21.4	49.0	27.7
	59.6	Pb	175	8.01	0.76		2.34	21.3	49.9	27.2
	59.0	Bi	436	8.01	0.74		1.78	21.2	50.3	26.2

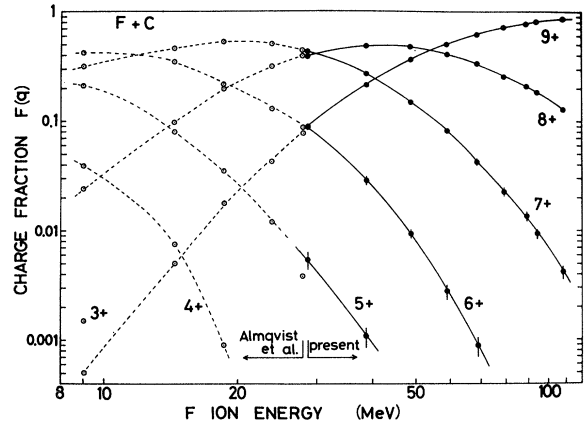

FIG. 2. Equilibrium charge-state fractions $F(q)$ of F ions obtained in this work (29—108 MeV) and by Almqvist *et al.* (9—28 MeV). Data are plotted as a function of exit energy from carbon foil.

target thickness to attain the charge-state equilibration must be known. For this purpose, nonequilibrium charge distributions were measured for the incidences of 61.3-MeV F^{8+} and 109-MeV F^{9+} ions on 3—148 $\mu g/cm^2$ carbon foils. Figure 1 shows the obtained charge-state fractions plotted as a function of carbon foil thickness. Figure 1 indicates that the use of 100-$\mu g/cm^2$ carbon foil is sufficient for the attainment of charge equilibration. Considering this result, foils greater than 100 $\mu g/cm^2$ thick were used.

In Fig. 2, equilibrium charge-state fractions $F(q)$ observed behind the carbon foil are plotted as a function of exit energy from the foil. The data by Almqvist *et al.* obtained below 28 MeV (Ref. 7) are also shown. Results of $F(q)$ as well as incident energy, exit energy from the foil, mean charge state $\bar{q}$, and charge-distribution width d are listed in Table I for 29—108-MeV F ions behind carbon foil. In Table II, results of Z_2-dependent charge states observed at the incident energies 30 and 60 MeV are shown. Here $\bar{q}$ and d are defined as

$$\bar{q}=\sum_q qF(q)\,, \tag{1}$$

$$d=\left[\sum_q (q-\bar{q})^2F(q)\right]^{1/2}. \tag{2}$$

The exit energies indicated in the tables have been estimated from the measured foil thickness multiplied by the stopping power given by Northcliffe and Schilling.[9] Experimental errors of $F(q)$, estimated from the statistics of monitor counts of scattered particles, the uncertainty of beam-current integration, and the reproducibility of measurement, are less than 2.5% for $F(q)>0.08$, 10% for $F(q)>0.01$, and 25% for $F(q)<0.01$. The errors coming from the target contamination as pointed out by several authors[4,10—12] are not taken into consideration.

III. VELOCITY DEPENDENCE OF F CHARGE STATES IN (29—108)-MeV F + C

In Fig. 3, mean charge states $\bar{q}$ of F ions after passage through carbon foils are plotted as a function of reduced velocity X (introduced by Nikolaev and Dmitriev[13]), which is defined as $X=v/(3.6\times10^8Z_1^{0.45})$, where v is the ion velocity in units of cm/sec. In Fig. 3, empirical formulas of $\bar{q}$ by Nikolaev and Dmitriev[13] (ND), To and Drouin[14] (TD), and by Shima, Ishihara, and Mikumo[5] (SIM) are drawn. The deduction of SIM is based on the fact that the predictions of other empirical formulas are systematically lower than those observed in the swift velocity region $X>1.5$. Such a trend is also seen for the present F ions, and observed data are almost reproduced by the formula of SIM.

In Fig. 4 charge-distribution widths d are plotted as a

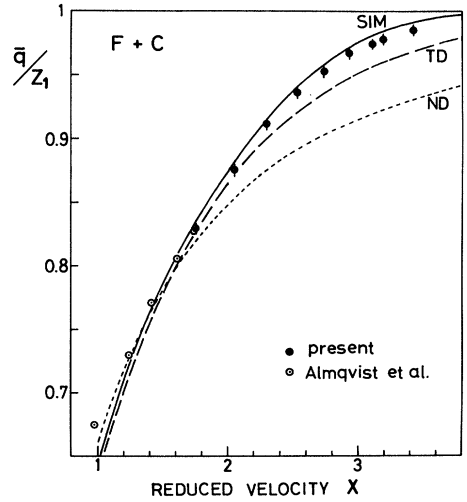

FIG. 3. Values of mean charge states $\bar{q}$ divided by $Z_1=9$ are plotted as a function of projectile reduced velocity $X=v/3.6\times10^8Z_1^{0.45}$, with v in cm/sec. SIM, TD, and ND stand for the empirical relations by Shima, Ishihara, and Mikumo, by To and Drouin, and by Nikolaev and Dmitriev, respectively.

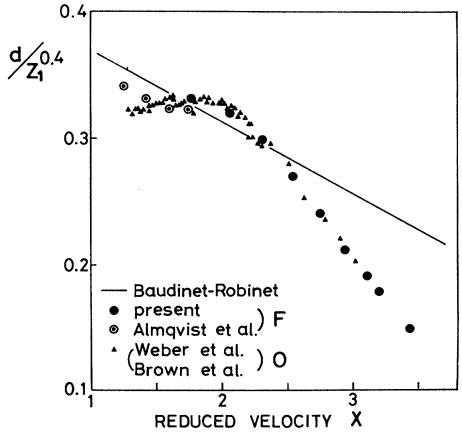

FIG. 4. Charge-distribution widths d divided by $Z_1^{0.4}$ are plotted as a function of reduced velocity X for F and O ions observed behind carbon foil. Solid straight line indicates the empirical relation [Eq. (3)] by Baudinet-Robinet.

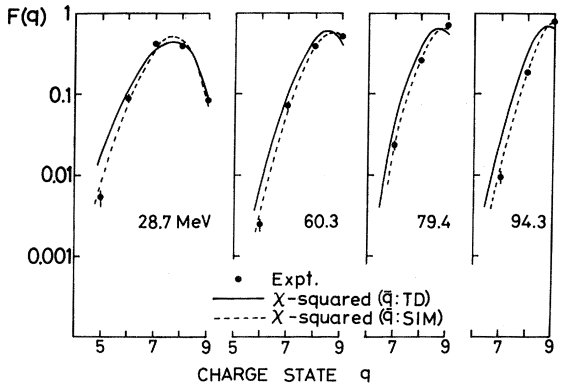

FIG. 5. Charge distributions of 28.7-, 60.3-, 79.4-, and 94.3-MeV F ions after passage through carbon foil. Solid and dotted curves indicate the reduced chi-squared distributions proposed by Baudinet-Robinet when empirical formulas of $\bar{q}$ by To and Drouin (TD) and by Shima *et al.* (SIM) are, respectively, used in the calculation.

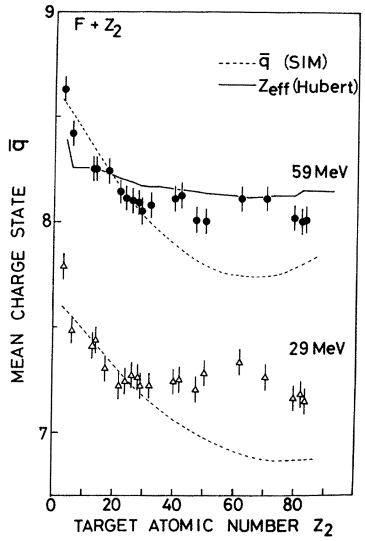

FIG. 6. Mean charge states $\bar{q}$ of F ions at the exit energies of 59 and 29 MeV are shown as a function of Z_2. Dotted lines indicate the $\bar{q}$ values from the empirical formula of SIM and solid line indicates the effective charge of F ions estimated from the stopping-power table by Hubert *et al.*

function of reduced velocity X. The reason to have taken the ordinate scale as $d/Z_1^{0.4}$ is because Baudinet-Robinet[15] reports on the empirical relation of d as

$$d = Z_1^{0.4}(0.426 - 0.0571X) . \quad (3)$$

Equation (3) is drawn with a solid line, which deviates from observed values at the swift velocity region. For comparison, the widths of F ions by Almqvist *et al.*[7] and the widths of O ions by Weber *et al.*[16] and by Brown *et al.*[17] observed behind the carbon foil are also plotted. Figure 4 indicates that d values decrease almost linearly with the increase of velocity of F and O ions at $X > 2$. In this velocity region charge-distribution functions become significantly asymmetric, and the width is influenced by the fractions of ions with a single electron (F^{8+}) and no electron (F^{9+}). On the other hand, the width becomes nearly independent of the projectile velocity at $X < 2$. In this region, as is seen in the following figure (Fig. 5), charge-distribution functions approach the symmetric function.

In Fig. 5, the distribution of charge-state fraction $F(q)$ is shown for projectile exit energies of 28.7, 60.3, 79.4, and 94.3 MeV. According to Baudinet-Robinet,[6,15] the charge distribution of highly ionized ions is approximated by the "reduced χ^2 distribution." In the numerical evaluation of this distribution, two quantities are necessary, i.e., the mean charge state $\bar{q}$ and the distribution width d which corresponds to the standard deviation. The solid line in Fig. 5 shows the reduced χ^2 distribution which is evaluated using the empirical formula by TD[14] for $\bar{q}$, and Eq. (3) for d. Observed distribution functions are seen to be fairly predictable using the reduced χ^2 distribution. It should be pointed out that the better agreement is obtained at the swift velocity region when the empirical formula of $\bar{q}$ by SIM[5] is used (dotted lines in Fig. 5) instead of that by TD. As was shown in Fig. 3, slight difference is seen in the values of $\bar{q}$ between SIM and TD. On the other hand, it was shown in Fig. 4 that the empirical relation of d by Baudinet-Robinet [Eq. (3)] significantly overestimates the observed values at the swift velocity region. However, the reduced χ^2 distribution is rather sensitive to the choice of $\bar{q}$ formula than the choice of d formula.

IV. Z_2 DEPENDENCE OF 29- AND 59-MeV F-ION CHARGE STATES

Charge-distribution data for various ${}_{Z_2}X$ foils have been measured at the common incident energies of F ions at 30 and 60 MeV. Consequently, projectile exit energies from foil differ according to different ${}_{Z_2}X$ foils (see Table II). Using the most simple empirical relation of $\bar{q} = Z_1[1 - \exp(-X)]$ given by TD,[14] obtained $\bar{q}$ values have been adjusted to the $\bar{q}$ values which are expected at the common exit energies of 29 and 59 MeV. Adjusted $\bar{q}$ values are plotted in Fig. 6 as a function of Z_2. Generally, the higher-charge states are observed for the passage through the lower-Z_2 foils. Within the foils tested at present, Be is the most efficient foil in obtaining the high-charge state. In the review article by Betz,[18] the existence of such trend was already pointed out by comparing the $\bar{q}$ values of S, Br, and I ions after passage through several ${}_{Z_2}X$ foils. In the case of present F ions, the observation of this trend has been confirmed with the use of as many as 20 kinds of ${}_{Z_2}X$ foils. Based on the existing data of several heavy ions showing the Z_2 dependence of $\bar{q}$, a Z_2-dependent empirical formula of $\bar{q}$ was presented by SIM[5] that is applicable to ions $Z_1 \geq 14$. In Fig. 6, the $\bar{q}$ values of SIM are drawn with dotted lines. The prediction of SIM, when applied to F ions, shows the systematic underestimation for foils $Z_1 > 40$ by 6% at maximum.

It is interesting to compare the Z_2 dependence of $\bar{q}$ and that of effective charge Z_{eff} estimated from stopping power. From the comparison of stopping powers of heavy

ions $(dE/dx)_{HI}$ and of light ions $(dE/dx)_{LI}$ at an equal velocity in the same material, effective charge of heavy ions $(Z_{eff})_{HI}$ is defined as

$$(Z_{eff})_{HI}/(Z_{eff})_{LI}=[(dE/dx)_{HI}/(dE/dx)_{LI}]^{1/2}, \quad (4)$$

where $(Z_{eff})_{LI}$ means the effective charge of light ions. $(Z_{eff})_{HI}$ values have long been considered to be almost independent of Z_2. In fact, effective charges in the stopping-power table of Northcliffe and Schilling[9] are taken to be independent of Z_2. However, according to the recent stopping-power measurement of Bimbot *et al.*[19,20] and Geissel *et al.*[21,22] at the swift ion velocities of several MeV/amu, effective charges exhibit the higher values for the lower-Z_2 material, and this trend becomes striking with increasing projectile energy. Based on the stopping-power data by Bimbot *et al.*, a stopping power table was presented by Hubert *et al.*[23] in the range of the projectile energies greater than 2.5 MeV/amu. Z_{eff} values of 59-MeV F ions estimated from the table of Hubert *et al.* are drawn with a solid line in Fig. 6. It should be noted that the similar Z_2-dependent behavior is seen between $\bar{q}$ and Z_{eff}. Z_{eff} is the quantity that reflects the degree of some excited charge state of ions inside the foil, while $\bar{q}$ is the ground-state mean charge behind the foil. Figure 6 indicates that the highly charged ions observed behind the foil are already in a highly excited state inside the foil. Since the definition differs between $\bar{q}$ and Z_{eff}, the comparison of them in absolute values is difficult. However, in spite of the use of solid target for the measurement of $\bar{q}$, quite a good agreement in the values of $\bar{q}$ and Z_{eff} is surprising. One reason for this is because, for 59-MeV F ions, charge fractions are dominated with F^{8+} and F^{9+} ions, and hence, the effect of charge state increase due to the post-foil Auger electron emission can be neglected.

In Fig. 7 are shown the charge-state fractions $F(q)$ of F ions after passage through Be, C, and Cu foils (upper), and the distribution widths d plotted as a function of Z_2 (lower). Although mean charge states differ according to Z_2, clear Z_2 dependence is not seen in the case of 30-MeV F-ion impacts. On the other hand, in the case of 60-MeV F-ion impacts, d values are seen to become narrow with decreasing Z_2, which corresponds to the increase of the fraction F^{9+} after passage through the lower-Z_2 foils (see the upper part of Fig. 7).

The interest in measuring the Z_2-dependent charge states has been in the investigation whether the Z_2 oscillation of $\bar{q}$ is observed or not in the F ions of swift velocities. In the $\bar{q}$ values of 30—110-MeV Si and 70- and 110-MeV Cl ions, Z_2 oscillation was clearly seen.[3] On the contrary, no obvious Z_2 oscillation has been observed in the $\bar{q}$ values of 29- and 59-MeV F ions although the ionic velocities of these three kinds of ions are of comparable magnitude. Many processes are involved and it is not easy to seek the exact reason for this result. One of the possibilities for the interpretation is described in the following.

In the $\bar{q}$-vs-Z_2 relation of Si and Cl ions, it was pointed out that the Z_2 positions exhibiting the maxima and minima of observed $\bar{q}$ correspond to those of the minima and maxima, respectively, of electron-capture cross sections into the projectile K vacancy. Furthermore, applying the method of Hopkins *et al.*,[24] the fractions of projectiles with K vacancies inside the foil were obtained for several $_{z_2}X$ foils, and the oscillation of the projectile fractions with single- or double-K vacancy with Z_2 was confirmed to exhibit the trend similar to the oscillation of $\bar{q}$ with Z_2. If we plot the calculated cross sections for electron loss [binary-encounter-approximation (BEA) cross sections[25]] and electron capture [Brinkman and Kramers (BK) cross

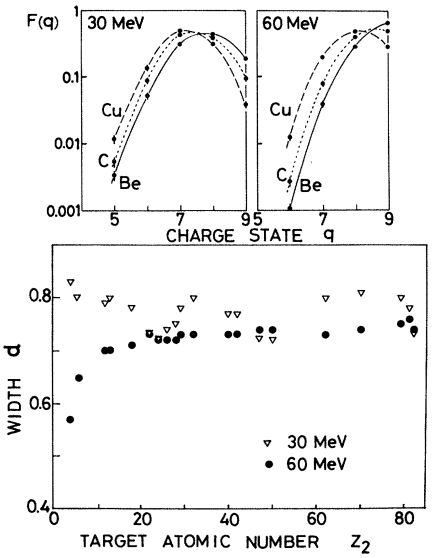

FIG. 7. Charge-state distributions of F ions after passage through Be, C, and Cu foils (upper) and charge-distribution widths of F ions vs Z_2. Projectile energies in the figures are all incident energies.

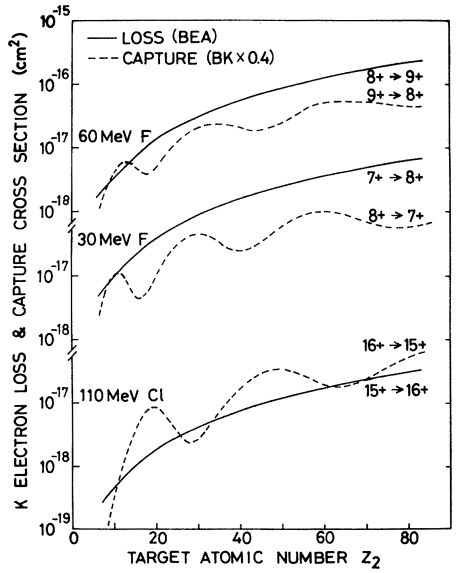

FIG. 8. Electron-loss and -capture cross sections of projectiles for collisions of 30- and 60-MeV F + $_{z_2}X$ and 110-MeV Cl + $_{z_2}X$. Solid curves indicate the loss cross sections calculated from BEA (binary-encounter approximation), and dashed curves indicate the capture cross sections calculated from BK (Brinkman and Kramers).

sections[26] multiplied by 0.4] in Fig. 8, electron-capture cross sections are seen to oscillate as a function of Z_2. Cross sections of projectiles in 60-MeV $F + {}_{Z_2}X$ ($F^{9+} \rightarrow F^{8+}$, $F^{8+} \rightarrow F^{9+}$), 30-MeV $F + {}_{Z_2}X$ ($F^{8+} \rightarrow F^{7+}$, $F^{7+} \rightarrow F^{8+}$), and 110-MeV $Cl + {}_{Z_2}X$ ($Cl^{16+} \rightarrow Cl^{15+}$, $Cl^{15+} \rightarrow Cl^{16+}$) are shown in the figure, where ionization potentials given by Carlson *et al.*[27] are used for the calculation. The reason for applying the reduction factor 0.4 to BK cross sections is that Nielsen *et al.*[28] measured the nonequilibrium charge states of F ions in 9—38-MeV F + C collisions, in which deduced capture and loss cross sections are, respectively, about 0.4 times as much as BK cross sections and about the same magnitude as the BEA cross sections. Figure 8 shows that the amplitude of the oscillation of capture cross sections in F ions is smaller than that in Cl ions. Moreover, electron-loss cross sections, which increase monotonically with increasing Z_2, dominate the capture cross sections in 30- and 60-MeV F ions. Consequently, in the case of F ions, the influence of Z_2 oscillation of capture cross sections on the equilibrated electron-loss and -capture process is relatively weak compared with the case of Cl ions, which is considered to be one of the reasons why Z_2 oscillation of $\bar{q}$ is not obvious in 29- and 59-MeV F ions. In the present swift F ions, the magnitude of deexcitation cross section $1/n v \tau$ (where n is the target atomic density, v the ion velocity, and τ is the lifetime of excited state of F ions) is much smaller than the magnitude of the electron-loss or -capture cross section. Therefore, only the loss and capture cross sections are compared in the above discussion. For the quantitative discussion, the competition of various processes including the excited states of ions in solid must be considered.

V. CONCLUSION

Equilibrium charge-state distributions of swift F ions have been measured behind thin foils, and ion-velocity dependence as well as Z_2 dependence of F-ion charge states has been investigated. Mean charge states of F ions behind carbon foil are reproduced by the empirical formula by Shima *et al.* Asymmetric charge-state distribution of F ions is well approximated by the reduced χ^2 distribution proposed by Baudinet-Robinet. Better agreement is especially obtainable when the SIM formula of $\bar{q}$ is adopted in the evaluation of reduced χ^2 distribution. Mean charge states of 29- and 59-MeV F ions behind 20 kinds of ${}_{Z_2}X$ foils have exhibited the higher values after passage through the lower-Z_2 foils. This trend is similar to that of the Z_2 dependence of effective charges estimated from stopping powers. Within the foils tested at present, Be is the most efficient foil to obtain the high-charge state. Contrary to the Z_2 oscillation of mean charge states reported in swift Si and Cl ions, obvious Z_2 oscillatory behavior has not been observed in F ions. One of the reasons for this is considered to be related with the fact that the amplitude of Z_2 oscillation of electron-capture cross sections into F K-shell vacancy is relatively small compared with that into Si and Cl K-shell vacancy.

ACKNOWLEDGMENTS

It is a pleasure to acknowledge the staff of Tandem Accelerator Center at the University of Tsukuba for their support during the experiment. Thanks are also due to K. Michikawa for his assistance in the preparation of foils.

[1]W. N. Lennard and D. Phillips, Phys. Rev. Lett. 45, 176 (1980).
[2]W. N. Lennard, D. Phillips, and D. A. S. Walker, Nucl. Instrum. Methods 179, 413 (1981).
[3]K. Shima, T. Ishihara, T. Momoi, T. Miyoshi, K. Numata, and T. Mikumo, Phys. Lett. 98A, 106 (1983).
[4]Y. Haruyama, Y. Kanamori, Y. Kido, A. Itoh, and F. Fukuzawa, J. Phys. B 16, (1983) 1225.
[5]K. Shima, T. Ishihara, and T. Mikumo, Nucl. Instrum. Methods 200, 605 (1982).
[6]Y. Baudinet-Robinet, Phys. Rev. A 26, 62 (1982).
[7]E. Almqvist, C. Broude, M. A. Clark, J. A. Kuehner, and A. E. Litherland, Can. J. Phys. 40, 954 (1962).
[8]T. Ishihara, K. Shima, T. Kimura, S. Ishii, T. Momoi, H. Yamaguchi, K. Umetani, M. Moriyama, M. Yamanouchi, and T. Mikumo, Nucl. Instrum. Methods 204, 235 (1982).
[9]L. C. Northcliffe and R. F. Schilling, Nucl. Data Tables A 7, 233 (1970).
[10]W. N. Lennard, T. E. Jackman, and D. Phillips, Phys. Lett. 79A, 309 (1980).
[11]Y. Kido and J. Kawamoto, Nucl. Instrum. Methods 202, 329 (1982).
[12]C. J. Sofield, C. J. Woods, N. E. B. Cowern, L. B. Bridwell, J. M. Butcher, and J. M. Freeman, Nucl. Instrum. Methods 203, 509 (1982).
[13]V. S. Nikolaev and I. S. Dmitriev, Phys. Lett. 28A, 277 (1968).
[14]K. X. To and R. Drouin, Nucl. Instrum. Methods 160, 461 (1979).
[15]Y. Baudinet-Robinet, Nucl. Instrum. Methods 190, 197 (1981).
[16]D. J. Weber, N. M. Hintz, and D. Dehnhard, Nucl. Instrum. Methods 124, 317 (1975).
[17]R. A. Brown, G. D. Symons, and I. Hall, Nucl. Instrum. Methods 58, 274 (1968).
[18]H. D. Betz, Rev. Mod. Phys. 44, 465 (1972).
[19]R. Bimbot, S. D. Negra, D. Gardes, H. Gauvin, A. Fleury, and F. Hubert, Nucl. Instrum. Methods 153, 161 (1978).
[20]R. Bimbot, D. Gardes, H. Geissel, T. Kitahara, P. Armbruster, A. Fleury, and F. Hubert, Nucl. Instrum. Methods 174, 231 (1980).
[21]H. Geissel, Y. Laichter, W. F. W. Schneider, and P. Armbruster, Nucl. Instrum. Methods 194, 21 (1982).
[22]H. Geissel, Gesellschaft fur Schwerionenforschung (Darmstadt) Report No. 82-12 (unpublished).
[23]F. Hubert, A. Fleury, R. Bimbot, and D. Gardes, Ann. Phys. (Paris) Suppl. 5, 1 (1980).
[24]F. Hopkins, J. Sokolov, and A. Little, Phys. Rev. A 15, 588 (1977).

[25]J. D. Garcia, R. J. Fortner, and T. M. Kavanaugh, Rev. Mod. Phys. 45, 111 (1973).
[26]H. D. Betz, Methods Exp. Phys. 17, 73 (1980).
[27]T. A. Carlson, C. W. Neston, Jr., N. Wasserman, and J. D. McDowell, At. Data 2, 63 (1970).
[28]P. T. Nielsen, N. Rud, K. Dybdal, and K. B. Nielsen, Phys. Rev. A 27, 1189 (1983).